Supplementary Data

Charge Transport Dynamics and Emission Response in Quantum-Dot Light-Emitting Diodes for Next-Generation High-Speed Displays

Jeong-Wan Jo[a,†], Yoonwoo Kim[a,†], Bo Hou[b], Sung-Min Jung[a,*], and Jong Min Kim[a]

[a] *Electrical Engineering Division, Department of Engineering, University of Cambridge, 9 JJ Thomson Ave, Cambridge, CB3 0FA, United Kingdom*

[b] *School of Physics and Astronomy, Cardiff University, 5 The Parade, Newport Road, Cardiff, Wales, CF 24 3AA, United Kingdom*

[†]These authors contributed equally: Jeong-Wan Jo and Yoonwoo Kim

[*]Corresponding author.

E-mail address: sj569@cam.ac.uk (Sung-Min Jung)

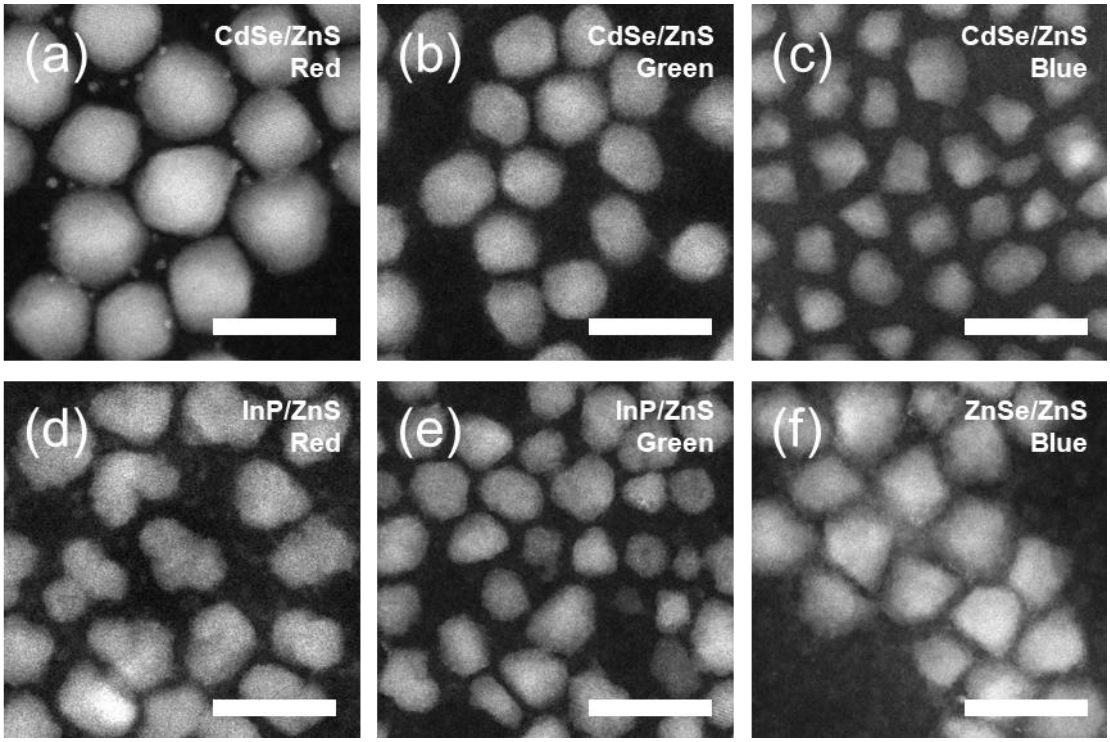

Fig. S1. Transmission electron microscopy (TEM) images for the CdSe/ZnS core/shell (a) red, (b) green, and (c) blue QD nanoparticles and for (d) InP/ZnS red, (e) InP/ZnS green, and (f) ZnSe/ZnS blue QD nanoparticles. Scale bars: 20 nm.

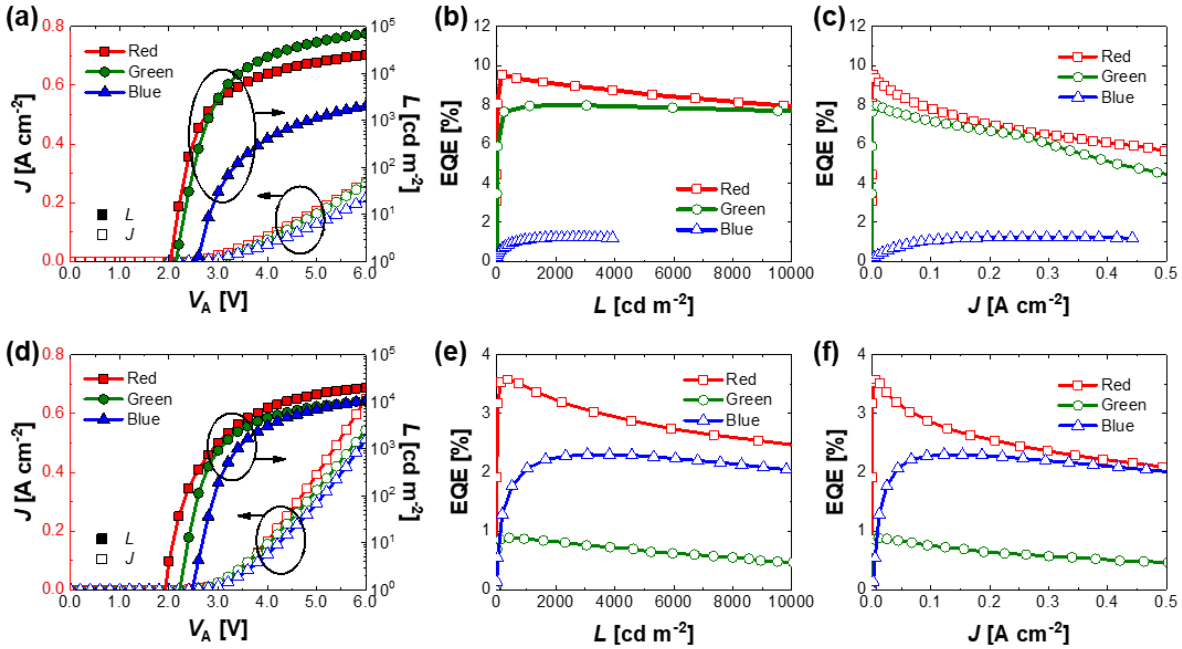

Fig. S2. Electro-optical properties of the fabricated red, green, and blue QD-LED devices. (a) Current density (J) – voltage (V_A) – luminance (L), (b) L – external quantum efficiency (EQE), and (c) J – EQE curves for Cd-based QD-LED devices. (d) J –V_A – L, (e) L – EQE, and (f) J – EQE curves for Cd-free QD-LED devices.

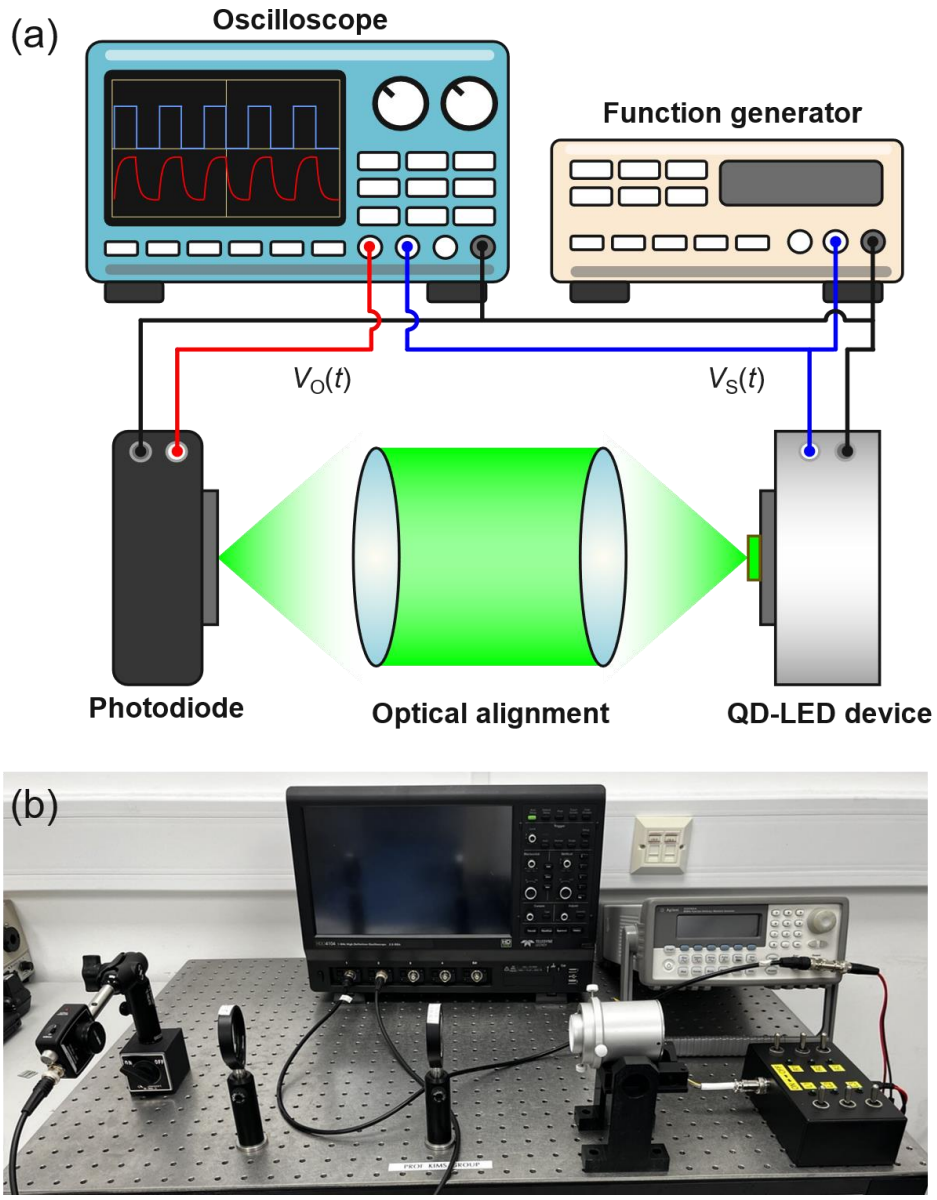

Fig. S3. Experimental setup for TrEL measurement. (a) schematic diagram of an optical experiment setup. A function generator drives a QD-LED device with a pulse signal voltage. The light emitted from the QD-LED device is transferred to the photodiode, by being focused through two optically aligned lenses. The spontaneous light emission is detected by a photodiode, and the signal is captured by an oscilloscope. $V_O(t)$ and $V_S(t)$ represent the voltage signals generated by the photodiode and function generator, respectively. (b) An experimental setup including an oscilloscope, function generator, optical components (lenses, photodiode, QD-LED device), and cable connections.

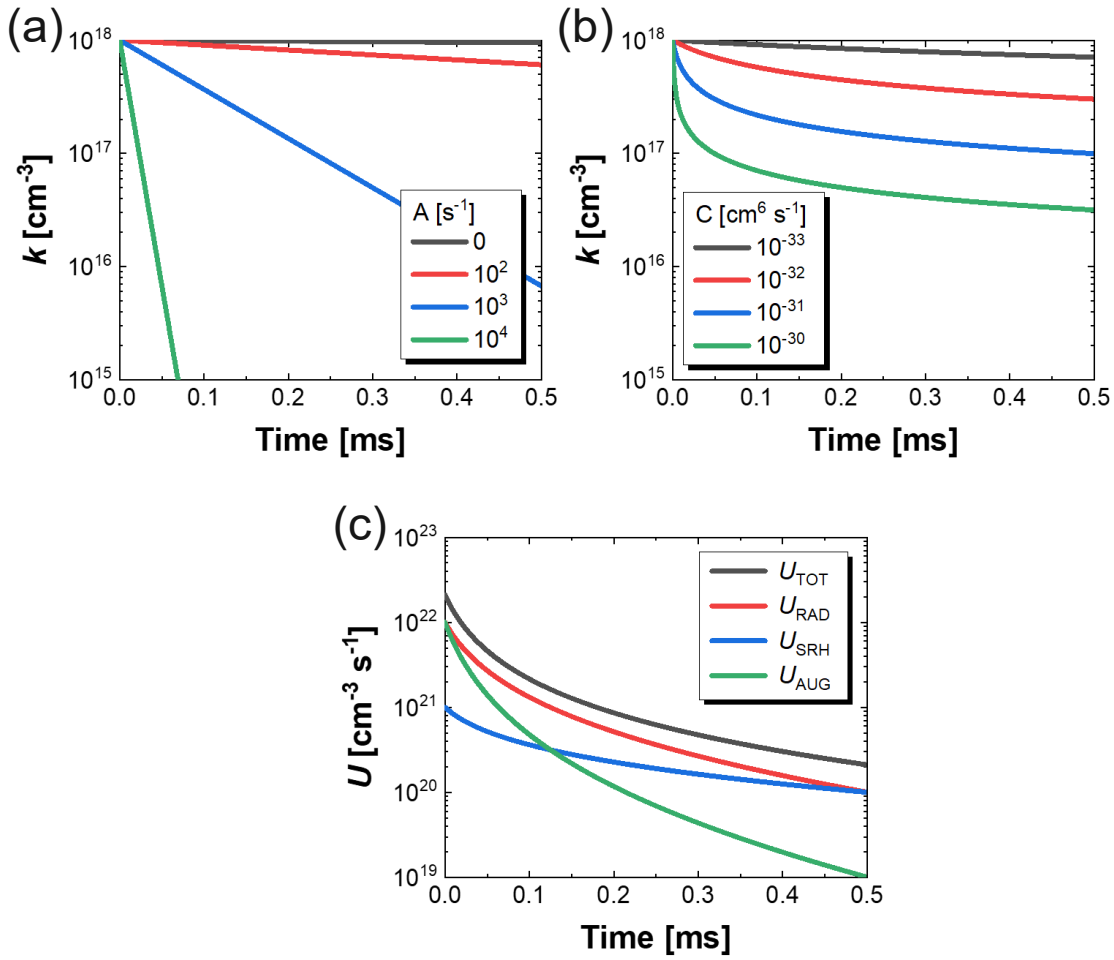

Fig. S4. Switching-off responses of carrier density and recombination rates within the EML of the QD-LED device under varying recombination parameters. (a) Theoretical evolution of carrier density over time after switching off the voltage, for different SRH recombination frequencies A, with Langevin recombination strength B = 0 cm^3 s^{-1} and Auger recombination probability C = 0 cm^6 s^{-1}. (b) Theoretical evolution of carrier density over time after switching off the voltage, for different Auger recombination probabilities C, with SRH recombination frequency A = 0 s^{-1} and Langevin recombination strength B = 0 cm^3 s^{-1}. (c) Recombination rate curves with SRH recombination frequency A at 10^3 s^{-1}, Langevin recombination strength B at 10^{-14} cm^3 s^{-1}, and Auger recombination probability C at 10^{-32} cm^6 s^{-1}.

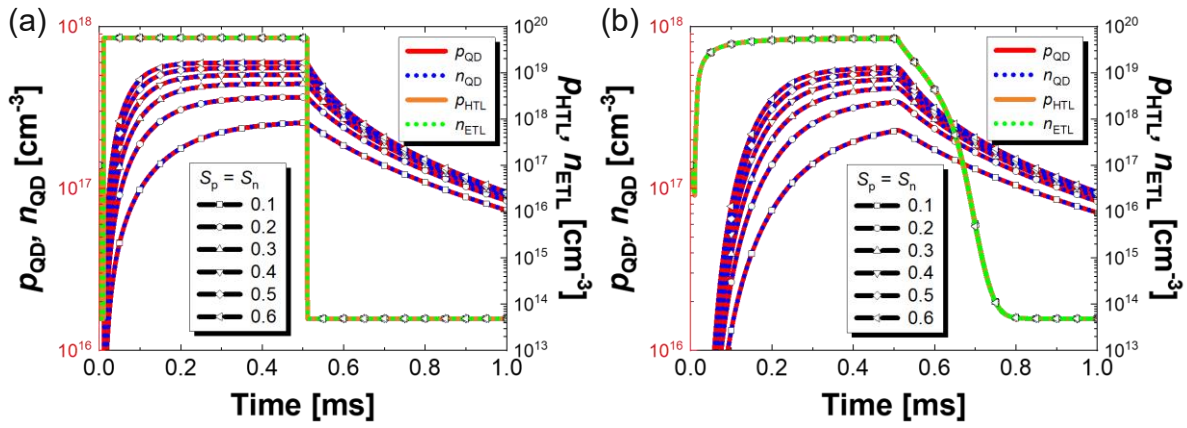

Fig. S5. Simulated carrier dynamics at the QD layer, and the HTL/QD and QD/ETL junctions. The red lines and blue dotted lines represent the hole and electron density at the QD layer, respectively. The orange lines and green dotted lines represent the hole at HTL/QD and electron density at QD/ETL interfaces, respectively. The carriers at the QD layer and interfaces are accumulated when the voltage is switched on and depleted when the voltage is switched off. (a) The scenario where the mobilities for holes in the HTL (μ_p^{HTL}) and electrons in the ETL (μ_n^{ETL}) are equal at 10^{-3} cm^2 V^{-1} s^{-1}. (b) The case with reduced mobilities of 10^{-6} cm^2 V^{-1} s^{-1} for both holes in the HTL and electrons in the ETL. The curves with different marks represent carrier injection coefficients S_n and S_p, affecting the on-response speed of the carrier accumulation at the QD layer.

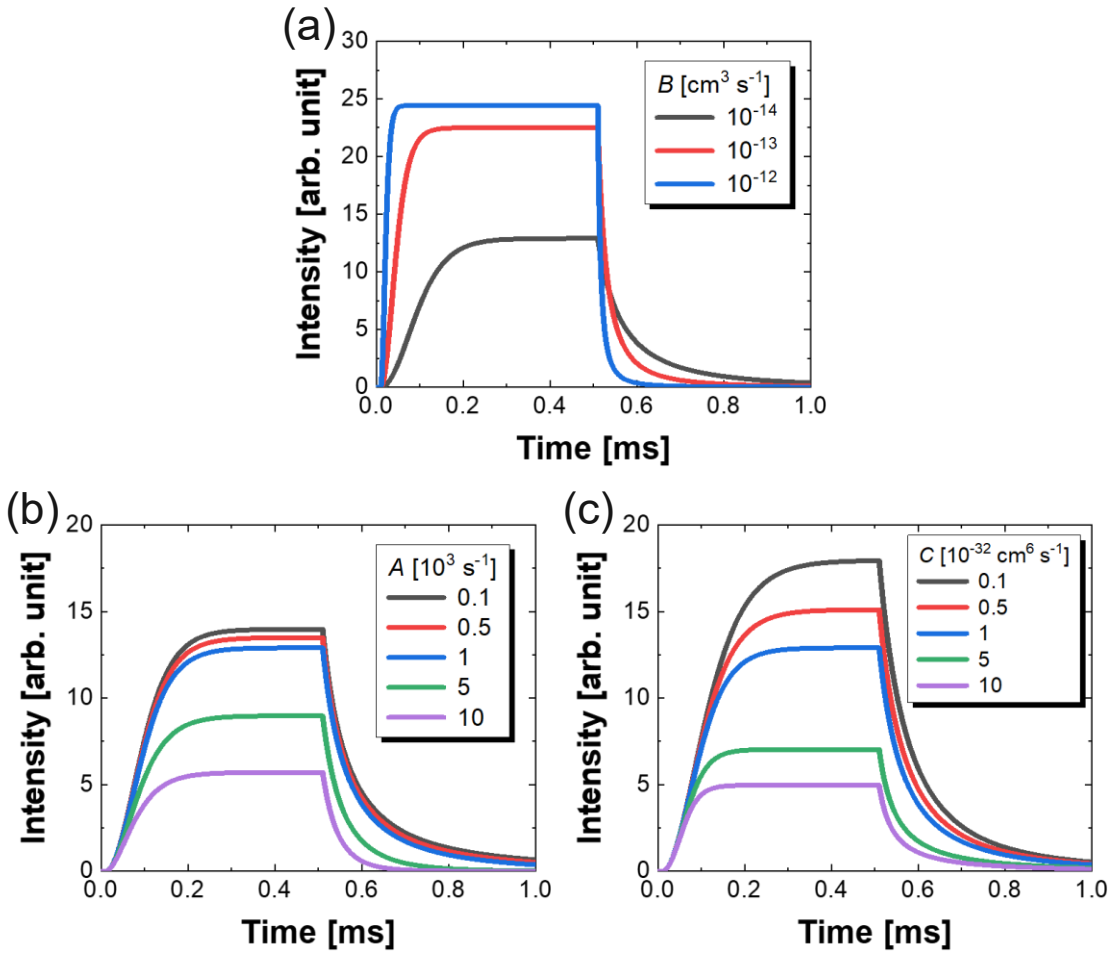

Fig. S6. Impact of recombination constants on emission response under charge-balanced conditions. The emission responses correspond to different (a) Langevin recombination coefficients *B*, (b) SRH recombination frequencies *A*, and (c) Auger recombination probabilities *C*. An increase in emission intensity is observed as the Langevin recombination coefficient *B* increases, indicating enhanced radiative recombination. Conversely, the emission intensity is diminished with higher values of the non-radiative SRH and Auger recombination parameters *A* and *C*, respectively.

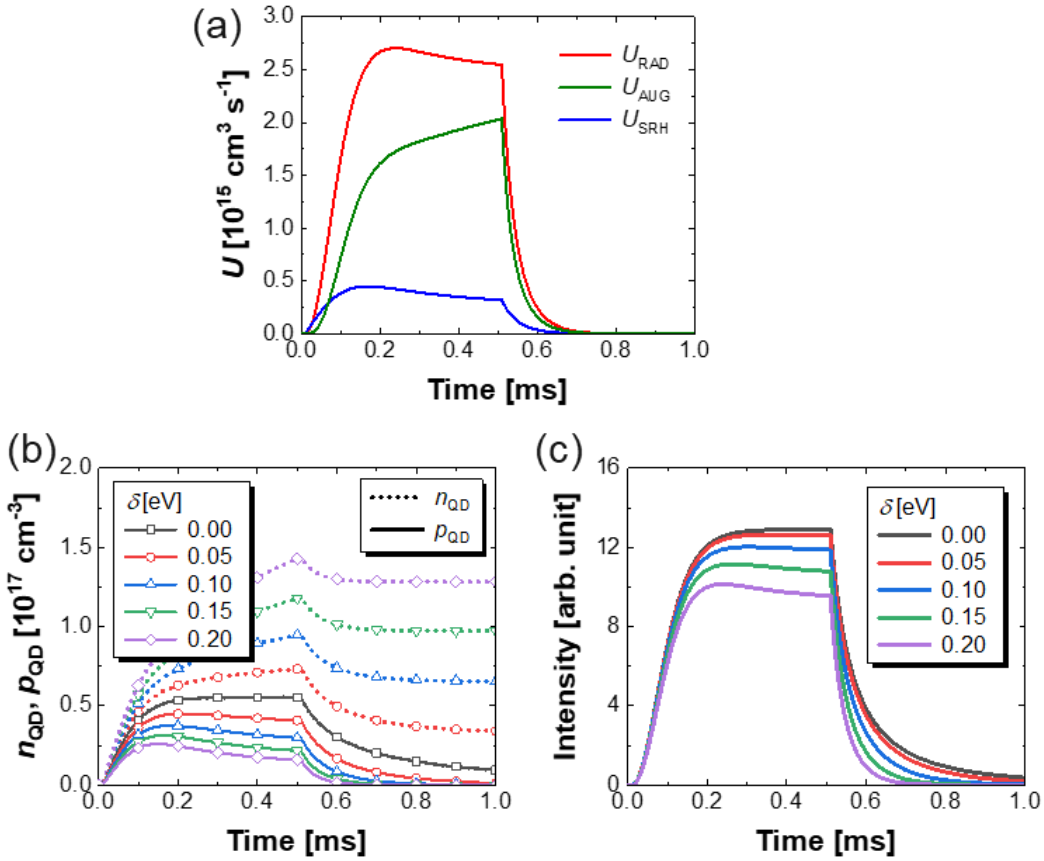

Fig. S7. Dynamic carrier densities and emission power under charge-imbalanced conditions. (a) Simulated time-dependent Langevin radiative, SRH and Auger non-radiative recombination rates. (b) Simulated hole (solid lines) and electron (dotted lines) densities at the QD layer, and (c) the emission intensities as a function of time, for various energy band misalignment parameters δ. As the band misalignment increases, the difference between the electron and hole densities at the QD layer increases, and the intensity drop becomes more serious.

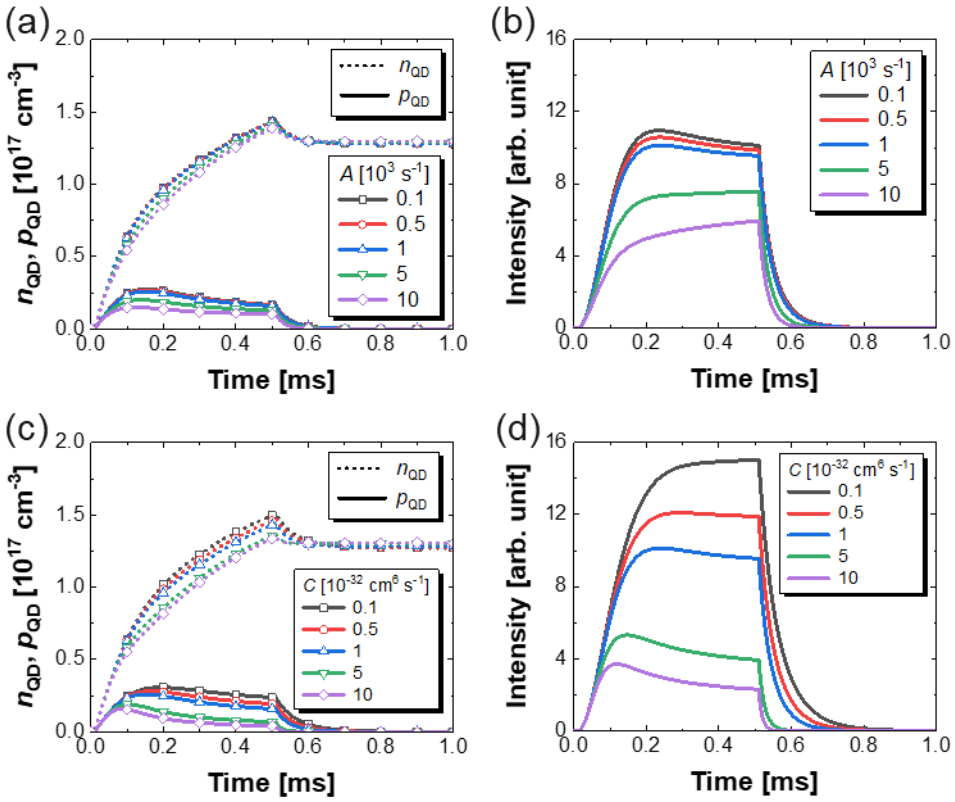

Fig. S8. Dynamic carrier densities and emission power under charge-imbalanced conditions. (a) Simulated hole (solid lines) and electron (dotted lines) densities at the QD layer, and (b) the emission intensity responses over time, for different SRH recombination frequencies A, with a fixed band misalignment parameter δ of 0.2 eV. (c) Simulated hole (solid lines) and electron (dotted lines) densities at the QD layer, and (d) the emission intensity responses over time, for various Auger recombination coefficients C, also at a fixed band misalignment δ of 0.2 eV.

Table S1. Material parameters of QDs used in the simulation.

QD Parameters	**Core**	**Shell**
Diameter [nm]	5.5	
Shell thickness [nm]		1.0
Number of QD layer		2
Dielectric constant ε_r	9.4	
Hole mobility μ_{p0}^{QD} [$cm^2\ V^{-1}\ s^{-1}$] @ F_0=5.0 [MV cm^{-1}]	10^{-6}	
Electron mobility μ_{n0}^{QD} [$cm^2\ V^{-1}\ s^{-1}$] @ F_0=5.0 [MV cm^{-1}]	10^{-6}	
Centre wavelength λ_0 [nm]	530	
Conduction band edge E_{C0} [eV]	3.63	-3.35
Optical Bandgap E_G [eV]	2.34	2.9
Langevin radiative recombination strength B [$cm^3\ s^{-1}$]	10^{-14}	
SRH non-radiative recombination frequency A [s^{-1}]	10^3	
Auger non-radiative recombination probability C [$cm^6\ s^{-1}$]	10^{-32}	
Charge injection coefficient $S_p = S_n$ for the hole and electron	0.5	

Table S2. Materials and device parameters of transport layers and electrodes of QD-LEDs used in the simulation.

Parameters	**Anode**	**HIL**	**HTL**	**ETL**	**Cathode**
Materials	ITO	PEDOT:PSS	TFB	ZnO	Al
Thickness [nm]		20	40	40	
Dielectric constant, ε_r		3.0	5.0	5.0	
Hole mobility, μ_p [$cm^2\ V^{-1}\ s^{-1}$]		3.2×10^{-4}	2.0×10^{-3}		
Electron mobility, μ_n [$cm^2\ V^{-1}\ s^{-1}$]				2.0×10^{-3}	
Doping type		p-type	p-type	n-type	
Doping concentrations, N_a, N_d [cm^{-3}]		2.8×10^{19}	1.0×10^{17}	1.0×10^{17}	
Work-functions, ϕ [eV]	4.7				4.0
Conduction band edge, E_{C0} [eV]		-3.60	-2.60	-4.00	
Valance band edge, E_{V0} [eV]		-5.17	-5.60	-7.40	